Songklanakarin J. Sci. Technol.
34 (5), 587-596, Sep. - Oct. 2012

SJST SONGKLANAKARIN JOURNAL OF SCIENCE AND TECHNOLOGY
http://www.sjst.psu.ac.th

Original Article

Simulation of sandstone degradation using large-scale slake durability index testing device

Chaowarin Walsri, Tanaphol Sriapai, Decho Phueakphum* and Kittitep Fuenkajorn

Geomechanics Research Unit, Institute of Engineering,
Suranaree University of Technology, Mueang, Nakhon Ratchasima, 30000 Thailand.

Received 6 January 2012; Accepted 30 June 2012

abstract

Large-scale slake durability index tests have been performed on Khok Kruat (KK), Phu Kradung (PK) and Phra Wihan (PW) sandstone. A rotating drum with a diameter of 64 cm and length of 40 cm was fabricated to accommodate ten rock fragments with a nominal size of 10 cm. Both large-scale and standard-testing were performed under dry and wet conditions. The large-scale test yields rock deterioration twice greater than the small-scale test, primarily due to the greater energy imposed on the rock fragments. The weight losses under wet condition are 12%, 8%, and 3% greater than under dry condition for KK, PK, and PW sandstones, respectively. After 10 test cycles the water absorption values for PW, KK and PK sandstones are 12%, 3%, and 2%, respectively. Rock degradation under the rapid cooling-heating cycles in the laboratory is about 18 times faster than under the field condition in the northeast of Thailand.

Keywords: slake durability, weathering, sandstone, water absorption, degradation

1. Introduction

Slake durability index test has long been used to identify the durability and water sensitivity of rocks as subjected to engineering requirements under in-situ conditions. The test has been widely accepted and standardized by the American Society for Testing and Materials (ASTM) in 1987 (ASTM D4644), and included as part of the ISRM suggested methods by the International Society for Rock Mechanics (Brown, 1981). Several investigators have utilized this method with a common goal of correlating the rock durability, and sometimes strength, with the chemical or mineral compositions and the state of weathering (e.g. Dhakal *et al.*, 2002; Fang and Harrison, 2001; Gokceoglu *et al.*, 2000; Koncagul and Santi, 1999; Oguchi and Matsukura, 1999; Oyama and Chigira, 1999; Phienwej and Singh, 2005; Tugrul, 2004). One remaining question is how good the test results obtained from small fragment samples (normally about 1.5 in) can represent the natural process of rock degradation under in-situ condition. Even though considerable amount of research relevant to rock durability and weathering effects have been conducted, an attempt at investigating the size effects of the tested rock fragments has never been reported.

The primary objective of this study is to investigate the weathering and degradation characteristics of some intact sandstone by performing large-scale slake durability index testing. The results are compared with those obtained from the ASTM standard method. An attempt at predicting the rock strength degradation with time has also been made. The results can be useful for the design considerations and long-term stability analysis of rock foundations, embankments, and support system (i.e. by explicitly considering rock degradation in the design parameters). By testing larger specimens, the results can also be applied to predict the durability of rock rip rap used to protect embankments of reservoirs, river banks and shorelines.

* Corresponding author.
Email address: phueakphum@sut.ac.th

2. Large-scale Slake Durability Device

A large-scale slake durability device has been fabricated. It is similar to the ASTM standard device except that the rotating drum is enlarged to the size of 640 mm in diameter and 400 mm long (Figure 1). It is about 4.5 times larger than the drum size specified by the standard. The mesh openings around the drum are 6 mm. The drum can accommodate 10 representative rock fragments with nominal sizes of 10×10×10 cm. It is secured on a steel frame and can be freely rotated in the trough. Note, that the standard sized drum specified by ASTM (D4644) has a diameter of 140 mm, 100 mm in length with the mesh openings of 2 mm.

3. Rock Samples

The rock samples selected for testing belong to three sandstone members; including Khok Kruat, Phu Kradung and Phra Wihan sandstones (hereafter called KKSS, PKSS and PWSS). These rocks are commonly found in the northeast of Thailand. They play a significant role on the long-term stability of slope embankments and engineering foundations. The uniaxial compressive strength of KKSS, PKSS and PWSS are 67.5, 71.3, and 68.6 MPa, respectively (Kemthong, 2006; Fuenkajorn and Kenkhunthod, 2010). Based on the rock material classification proposed by ISRM using the uniaxial compressive strength (Brown, 1981; Singh and Goel, 1999), they can be classified as strong rocks, and are likely to deteriorate quickly after exposed to atmosphere. The rock fragments with nominal sizes of 3.81 cm (for standard testing) and 10 cm (for large-scale testing) were collected from the sites. Two sets of the samples were prepared for both sizes; one for dry testing and the other for wet testing. Each set comprised 10 fragments (Figure 2). Comparisons of the test results obtained from the two different sizes and under different test conditions would reveal the size effect on the rock deterioration and the water sensitivity of the sandstones. The mineral compositions of these rocks were identified by petrographic analyses. The results are given in Table 1.

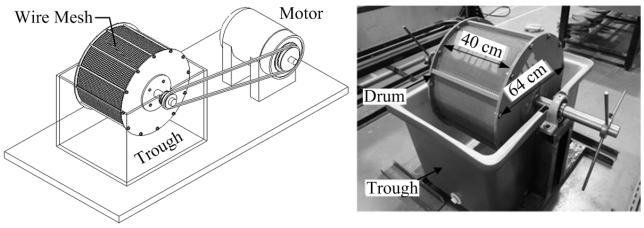

Figure 1. Drum constructed for large-scaled slake durability test.

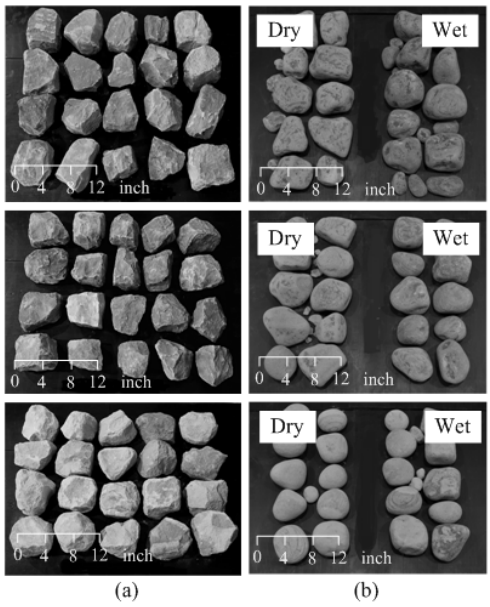

Figure 2. Rock samples before (a) and after testing (b). From top to bottom: Khok Kruat, Phu Kradung and Phra Wihan sandstone.

Table 1. Mineral compositions of rock specimens.

Mineral Compositions	KKSS	PKSS	PWSS
Quartz (%)	72.0	90.0	97.0
Mica (%)	3.0	2.0	-
Feldspar (%)	5.0	5.0	-
Kaolinite (%)	-	-	-
Calcite (%)	-	-	-
Halite (%)	-	-	-
Other (%)	20.0	3.0	3.0
Density (g/cm^3)	2.45	2.59	2.35
Cementing	calcite	hematite	silica
Contact	grain support	grain support	grain support
Grain size (mm)	0.1-1.5	0.1-1.0	2.0
Grain shape	angular	angular	angular
Shorting	poorly	moderate	well
Color	brownish red	brownish red	yellow

4. Slake Durability Test

4.1 Test method

For the 3.81-cm rock fragments, two series of slake durability index (SDI) tests were performed on two separate sets of rock specimens with similar and comparable characteristics. For the first series, the test procedure and data reduction were similar to that of the standard practice (ASTM D4644), except that the tests were performed up to six cycles (6 days), instead of two cycles as specified by the standard. This was primarily to establish a longer trend of weight loss as the rock continued to subject to more cycles of scrubbing in the drum. Temperature of the water in the trough was 25°C. The drum was turned 20 revolutions per minute for 10 minutes. The second test series was identical to the first one except that there was no water in the trough during rotating the drum, i.e., slaking under dry condition. The test was intended to assess the impact of water on the weathering process for each rock type. The dry-testing specimens were placed in the oven for 24 hrs for each cycle. Before testing they were cooled down to ambient temperature. The weight loss calculation for both wet and dry testing follows the ASTM (D4644-08) standard practice. The water absorption of rock specimens under degradation simulation in laboratory test and under actual conditions was determined using the ASTM (D6473-10; C127-04) standard test method.

Similar to the 3.81-cm fragments, the 10-cm rock fragments (large-scale testing) were also tested for two series using the large-scale testing drum. The testing was performed on two separate sets of rock specimens that have similar and comparable characteristics. Ten cycles of testing were performed for both wet and dry conditions. For each cycle, the drum was turned 20 revolutions per minute for 10 minutes. Figure 2 shows the rock fragments after testing.

4.2 Test results

Table 2 gives the SDI results for large-scale testing. The SDI values are plotted as a function of the test cycle (N) in Figure 3. The greater reduction of the SDI values was obtained for the large-scale testing, as compared to the standard scale testing. This is primarily due to the greater energy imposed to the large rock fragments.

It seems that all tested sandstones were sensitive to water. The SDI reduction rates for wet testing were greater than those for dry testing. At the end of cycle 10 the SDI values for wet testing were clearly lower than those for dry testing for all sandstones (Figure 4). Khok Kruat sandstone showed greater water sensitivity than the other two.

Figure 5 shows the water absorption as a function of test cycles (N). They were measured from the rock fragments used in the wet testing. The ability to absorb water of the sandstone fragments reduced as the number of test cycles increases. This implies that before testing the outer matrix of the rock fragments was weathered more than the inner portion. As the test cycle increased the scrubbing process slowly removed the outer matrix and exposes the fresher inner matrix to the testing environment. The inner matrix was comparatively fresh and had lesser amounts of pore spaces as compared to the outer part.

5. Implications of SDI on Long-term Durability

An attempt was made here to project the results of the SDI testing toward the future conditions of the rocks. A hypothesis was proposed to describe the physical characteristics of the rock fragments used in the SDI test. It was assumed that all rock fragments inside the drum for each test were identical. Figure 6 shows two different types of the rate of degradation (weight loss) during the SDI testing.

The first type shows relatively linear decreases of the SDI as the number of test cycles increases (Figure 6a). This indicates that each rock fragment in the drum had a relatively uniform texture (uniform degree of weathering, hardness or strength) from the inner matrix to the outer surface. The lower the strength of the rock fragment, the higher the rate of degradation.

Table 2. Slake durability index (SDI) for large-scaled testing.

Rock Types	Slake Durability Index (%)									
	Number of Cycles (N)									
	1	2	3	4	5	6	7	8	9	10
Wet testing										
KKSS	93.68	89.98	87.13	84.54	81.72	79.07	76.70	74.29	72.28	70.22
PKSS	95.42	92.44	90.39	88.16	86.30	84.49	82.79	81.21	79.63	78.15
PWSS	92.84	87.57	83.77	80.14	76.17	72.76	70.10	68.18	65.96	63.14
Dry testing										
KKSS	95.60	93.67	91.92	90.23	88.10	86.94	85.41	84.11	83.31	82.39
PKSS	96.01	94.27	92.89	91.20	90.23	88.93	87.94	87.28	86.49	85.68
PWSS	93.87	90.38	87.05	83.88	80.49	77.08	74.23	71.36	68.55	65.70

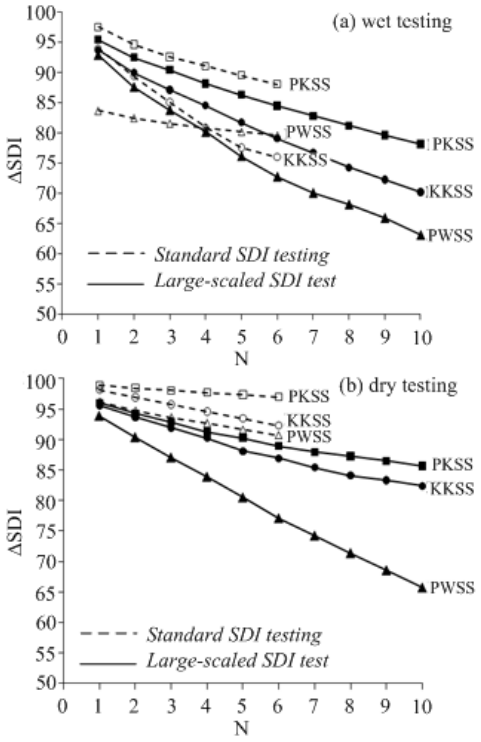

Figure 3. Results of SDI tests: wet (a) and dry testing (b).

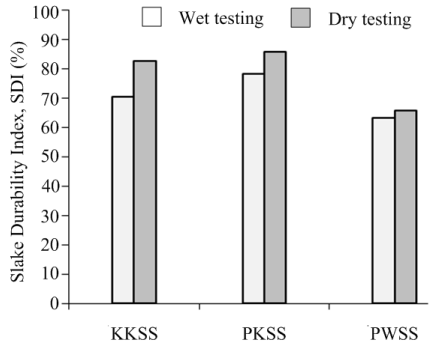

Figure 4. SDI at cycle no.10 for wet and dry testing.

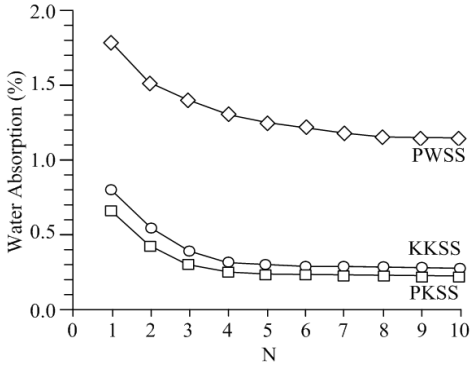

Figure 5. Water absorption as a function of test cycles.

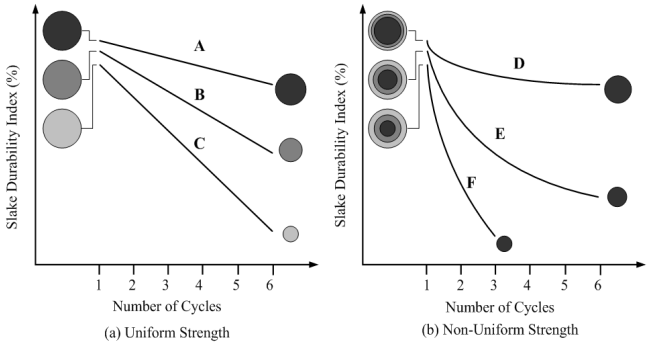

Figure 6. Proposed concept of rock degradation during SDI testing. Samples A, B and C (a) have uniform texture. Samples D, E and F (b) have weathered zone outside and fresher matrix inside.

For the second type (Figure 6b) each rock fragment inside the drum had a non-uniform texture. The outer surface was weaker (lower strength, higher degree of weathering, or more sensitive to water) than the inner matrix. This was reflected by the decrease of the rate of degradation as the test cycles increase and the curves for samples D, E and F are concave upward. Here, the decrease of the rock matrix strength from the outer surface to the inner part could be abrupt or grading, depending on the rock type and weathering characteristics. The more abrupt the change, the more concave is the SDI-N curve. It is believed that weathering characteristics of most rocks follow the second type, because the SDI-N curves obtained here and from elsewhere tend to be concave, more or less, upward.

6. Projection of Rock Durability

Let us assume here that the proposed hypothesis of the second type of weathering (Figure 6b) is valid. It can be postulated that rock fragments inside the drum tend to get stronger as they are subjected to a larger number of SDI test cycles. When the rock fragments become stronger, the difference in the SDI values between the adjacent cycles (hereafter called ΔSDI) becomes smaller. In order to predict the rock durability in the future, the ΔSDI values are calculated for the tenth cycles. Figure 7 plots the ΔSDI as a function of the reversed cycles, N*. This is primarily to avoid confusion with the original forward cycles (N) defined earlier. This reversed plotting is mainly for a convenience in analyzing the test results. For example, the ΔSDI that represents the difference between the SDI of the first cycle (I_{N1}) and the conditions as collected or before testing (I_{N0} = 100) is plotted at N* = 10. The difference of the SDI values of the ninth (I_{N9}) and tenth (I_{N10}) cycles is plotted for N* = 1. Table 3 gives the ΔSDI calculated for N* using large-scale testing device. For this new approach, as the ΔSDI increases with N*, the rock becomes weaker. This is similar to the actual rock degradation due to the weathering process that probably occurs under in-situ condition.

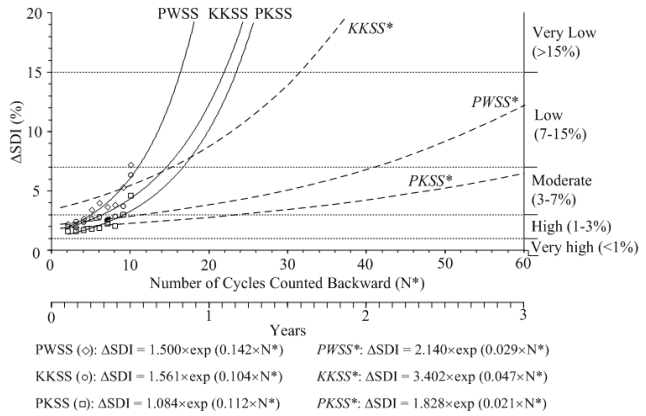

Figure 7. ΔSDI as a function of N*. Dash-lines obtained from Sri-in and Fuenkajorn (2007) and solid lines obtained from large-scaled slake durability test under wet conditions.

The ΔSDI–N* curves have a significant advantage over the conventional SDI–N diagram. The new curves can show a future trend for the rock durability, as ΔSDI values can be statistically projected to a larger number of test cycles beyond those performed in the laboratory. In Figure 7, the ΔSDI is projected to N* = 60 cycles. Regression analyses on the 10 ΔSDI values indicate that an exponential equation can best describe the variation of ΔSDI with N*. The implications of N* and the actual time or duration for which the rock is subject to actual in-situ conditions is very difficult to define, if at all possible. Table 4 gives the empirical relationship and summarizes the constants obtained for each rock type. Results in Figure 7 are useful for predicting rock degradation as a function of time.

7. Proposed Classification System for Rock Durability

A classification system is proposed for rock durability based on ΔSDI and its projected values to any N*, as shown in Table 5. The ΔSDI–N* curves obtained from three sandstones tested here are compared with the new classification system (Figure 7). For example, at N* = 60 or below, the result on 3.8-cm rock fragments (standard slake durability test) indicated that these three sandstones are classified as low to very low durability rocks. They are however classified as very low durability rocks when using 10-cm rock fragments (large-scale slake durability test), because their ΔSDI values rapidly increase within a few cycles of N*. It should be noted that the projection of ΔSDI–N* curves relies on the number of cycles actually tested. A larger number of tested cycles may result in a higher reliability of the projected results.

8. Correlation between Simulation and Actual In-situ Condition

An attempt is made here to correlate the simulation cycles with the actual in situ condition. The concept proposed by Sri-in and Fuenkajorn (2007) is adopted here. They state that an easy and relatively conservative approach to compare rock deterioration under different states is to use the concept of energy adsorption. The amount of heat energy that has been applied to the rock specimens during the degradation simulation is compared with those actually monitored in the northeast of Thailand throughout the year (Thai Meteorological Department, 2004). The heat energy absorbed by the rock can be calculated by using the following equation (Richard *et al.*, 1998).

$$Q = \sum_{i=1}^{n} \left(m \cdot C_p \cdot \Delta T_i \cdot \Delta t_i \right) \quad (1)$$

where Q is the absorbed energy of the rock specimen (kJ), m is the mass of rock specimens (kg), C_p is the specific heat capacity (kJ/kg·K), ΔT_i is the temperature change in Kelvin degrees, Δt_i is the time interval of energy absorption (hours) and n is the number of hours. The coefficient of heat capacity of most rocks varies between 0.6 and 1.2 kJ/kg·K with an average value of 0.90 kJ/kg·K. In the above equation, the absorbed energy during heating simulation of most rocks is estimated as 12.96 MJ·hr (where m = 15 kg, C_p = 0.90 kJ/kg·K, ΔT = 80 K, t = 12 h). For the in situ condition, the absorbed energy in one day is estimated as 0.735 MJ h (where m = 15 kg, C_p = 0.90 kJ/kg·K, ΔT is temperature change in each hour, and, t = 16 hours). Therefore, one simulation cycle of heating and cooling approximately equals 18 days under in-situ conditions (12.96/0.735 = 17.63). Therefore, n can be correlated with time, as n ≈ 18 days. This correlation is considered conservative because the temperature changes for the simulation are much more abrupt than those actually occurring under in-situ conditions. As the applied energy in one day during the simulation is the same as that used in the SDI test, N* can be related to time, as N* ≈ 18 days. The DSDI for each rock type shown in Figure 7 can therefore be calculated as a function of time.

Table 3. ΔSDI calculated for N* using large-scaled testing device.

Rock Types	Number of Cycles Counted Backwards (N*)									
	1	2	3	4	5	6	7	8	9	10
	I_{N9}-I_{N10}	I_{N8}-I_{N9}	I_{N7}-I_{N8}	I_{N6}-I_{N7}	I_{N5}-I_{N6}	I_{N4}-I_{N5}	I_{N3}-I_{N4}	I_{N2}-I_{N3}	I_{N1}-I_{N2}	100-I_{N1}
KKSS	2.06	2.01	2.41	2.37	2.65	2.82	2.59	2.85	3.70	6.32
PKSS	1.48	1.58	1.58	1.70	1.81	1.86	2.23	2.05	2.98	4.58
PWSS	2.82	2.22	1.92	2.66	3.41	3.97	3.63	3.80	5.27	7.16

Table 4. Comparison of the empirical constants for exponential relationship between DSDI and N* for the standard and large-scaled tests.

Rock Types	DSDI = A×exp[B×N*]		Correlation Coefficient
	A	B	
*Standard Slake Durability Test (ASTM D4644-87)			
KKSS	3.402	0.047	0.999
PKSS	1.828	0.021	0.999
PWSS	2.140	0.029	0.999
Large-Scaled Slake Durability			
KKSS	1.561	0.104	0.717
PKSS	1.084	0.112	0.776
PWSS	1.500	0.142	0.891

*From Sri-in and Fuenkajorn (2007)

Table 5. Proposed classification system for durability of intact rocks.

Description	ΔSDI (%)
Very high durability	< 1
High durability	1–3
Moderate durability	3–7
Low durability	7–15
Very low durability	> 15

9. Simulation and Verification of Rock Degradation

An attempt to verify the above hypothesis has been made by performing additional tests to simulate the rock degradation both in the laboratory and under actual conditions (or actual environment). Two set of rock specimens were prepared for these three sandstones; the cylindrical disks (50 mm diameter with 50 mm length) and rock fragments. They were separated into two test series for testing in the laboratory and under actual conditions. Figure 8 shows some of cylindrical rock specimens prepared for testing.

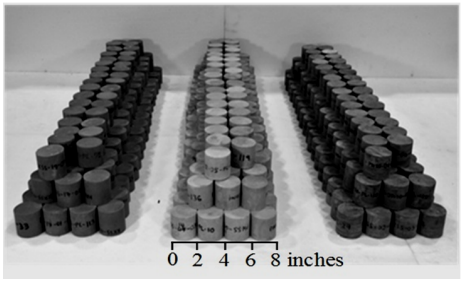

Figure 8. Rock samples prepared for tests: (from left to right) Khok Kruat, Phra Wihan and Phu Kradung sandstone.

For the laboratory simulation the specimens were placed in an oven at 110°C for 12 hrs and rapidly submerged in a tank of water at 25°C for 12 hrs. This rapid heating and cooling process was repeated 200 times (200 days). The physical properties (weight loss, specific gravity, and water absorption) of the rock fragments and the mechanical properties (uniaxial compressive strength and elastic modulus) of cylindrical specimens are monitored at every 20 cycles. The procedure follows the standard practice (ASTM C127-04 and ASTM D7012-04). Similar to the laboratory simulation, the other set of rock samples were placed outdoor subjected to the actual environment for 16 months (Figure 9). Every four months some samples are selected to measure their physical and mechanical properties. The results obtained from the two separated simulations are compared to assess the rock degradation. Figure 10 and 11 show the uniaxial compressive strength test and the post-test rock specimens.

Tables 6 and 7 summaries the physical properties of rock fragments obtained from laboratory simulation and actual in-situ conditon. The weight loss, water absorption

Figure 9. Rock samples placed under actual conditions.

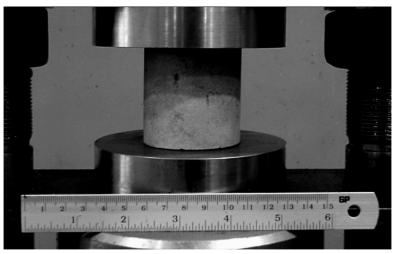

Figure 10. Uniaxial compressive strength test arrangement.

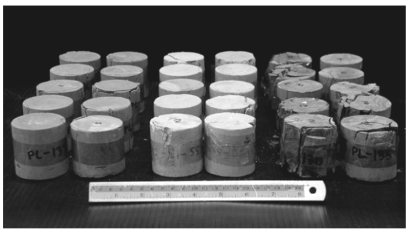

Figure 11. Some post-test samples (from the left to right) of KKSS, PWSS and PKSS.

Table 6. Dry density, water absorption, and weight loss of rocks for degradation simulation in the laboratory.

Cycle No.	Days	Dry Density (g/cm^3)			Water Absorption (%)			Weight Loss (%)		
		KKSS	PKSS	PWSS	KKSS	PKSS	PWSS	KKSS	PKSS	PWSS
0	0	2.55	2.69	2.38	0.10	0.05	0.16	0.00	0.00	0.00
20	20	2.54	2.68	2.38	0.20	0.20	0.40	0.49	0.33	0.52
40	40	2.53	2.67	2.36	0.50	0.40	0.80	0.71	0.46	0.60
60	60	2.52	2.66	2.36	0.80	0.70	1.10	1.09	0.99	0.85
80	80	2.53	2.66	2.35	1.10	0.90	1.40	1.57	1.14	1.05
100	100	2.53	2.66	2.35	1.30	1.00	1.70	1.80	1.57	1.53
120	120	2.52	2.66	2.34	1.60	1.20	1.90	2.20	1.90	1.81
140	140	2.51	2.66	2.33	1.80	1.40	2.10	2.42	2.05	2.01
160	160	2.50	2.66	2.33	1.90	1.60	2.30	2.53	2.27	2.63
180	180	2.50	2.65	2.32	2.10	1.80	2.50	2.94	2.65	2.79
200	200	2.49	2.64	2.31	2.30	2.10	2.70	3.45	3.17	2.99

Table 7. Dry density, water absorption, and weight loss of rocks for degradation simulation under actual condition.

Days	Dry Density (g/cm^3)			Water Absorption (%)			Weight Loss (%)		
	KKSS	PKSS	WSSP	KKSS	PKSS	PWSS	KKSS	PKSS	PWSS
0	2.55	2.69	2.38	0.10	0.05	0.16	0.00	0.00	0.00
120	2.50	2.67	2.34	0.45	0.19	0.33	1.03	0.86	1.08
240	2.46	2.65	2.30	0.68	0.23	0.45	1.83	1.68	1.89
360	2.45	2.63	2.29	0.84	0.34	0.56	2.68	2.41	2.78
480	2.44	2.60	2.27	1.02	0.45	0.72	3.15	2.90	3.30

and specific gravity of rock are presented as function of time. The results show that the rates of weight loss and water absorption of rock specimens simulated in the laboratory are higher than those subject to the actual conditions (Figures 12 and 13). The specific gravity for all three rock types deceased slowly at approximately the same rate both laboratory and actual condition (Figure 14). Tables 8 and 9 summaries the mechanical properties of cylindrical specimens obtained from laboratory simulation and actual in-situ condition. The uniaxial compressive strengths simulated in the laboratory and actual conditions decreased rapidly during the first cycle, and thereafter tended to decease at a lower rate (Figure 15). The elastic moduli measured from the two conditions were similar (Figure 16). The rock degradation in the laboratory tended to be greater than that under the actual conditions, as evidenced by the increasing of water absorption and weight loss and the decreasing of the rock compressivestrengths.

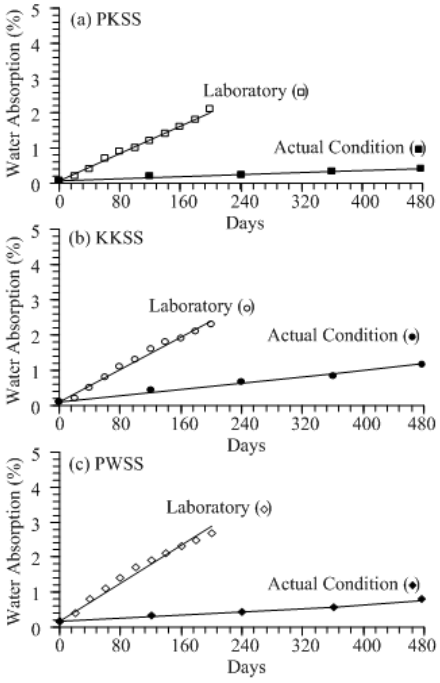

Figure 12. Water absorption as a function of time under degradation simulation in laboratory and under actual conditions.

10. Discussions and Conclusions

The large-scale laboratory test induces rock deterioration twice faster than the small-scale test. All tested sandstones showed a greater percentage of weight loss when they

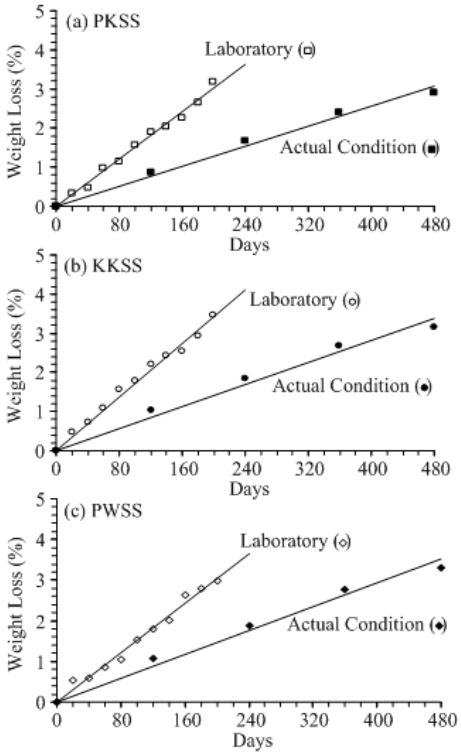

Figure 13. Weight loss as a function of time under degradation simulation in laboratory and under actual conditions.

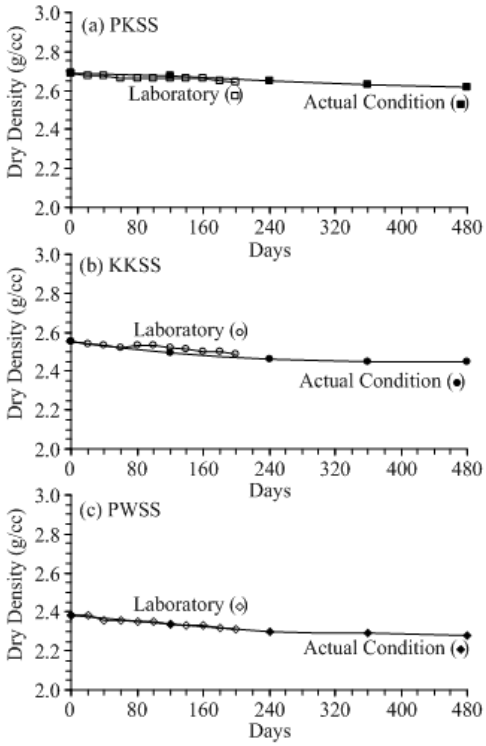

Figure 14. Density as a function of time under degradation simulation in laboratory and under actual conditions.

Table 8 Uniaxial compressive strengths and elastic moduli of rocks for degradation simulation in the laboratory.

Cycle No.	Days	Uniaxial Compressive Strength (MPa)			Elastic Modulus (GPa)		
		KKSS	PKSS	PWSS	KKSS	PKSS	PWSS
0	0	67.1±4.5	84.1±4.1	66.8±13.9	11.8±2.5	12.3±4.1	11.2±3.3
20	20	49.9±11.4	64.9±12.6	47.6±7.2	11.3±3.5	11.9±4.2	10.7±2.5
40	40	42.5±10.6	62.9±9.8	41.5±7.6	10.8±2.1	11.5±3.2	10.3±3.9
60	60	39.4±8.7	57.6±8.0	37.1±5.0	10.4±1.3	11.2±3.1	9.7±3.9
80	80	37.2±11.6	54.1±10.8	35.9±9.3	10.0±3.8	11.1±3.1	9.4±2.5
100	100	37.3±5.1	52.6±13.9	33.5±9.1	9.7±3.2	10.8±3.0	8.9±2.0
120	120	36.8±10.6	52.1±11.3	32.5±8.2	9.5±2.7	10.6±3.9	8.6±3.8
140	140	34.3±6.2	51.8±8.0	30.1±8.2	9.3±2.4	10.6±3.8	8.4±1.6
160	160	33.3±11.0	51.0±5. 2	29.9±6.9	9.2±2.2	10.4±2.9	8.2±3.5
180	180	34.1±4.3	49.0±13.1	29.4±6.4	9.1±1.3	10.3±3.2	8.1±2.8
200	200	33.9±8.6	48.8±8.1	27.6±5.6	9.1±1.7	10.3±3.5	8.1±3.2

were tested by using 10 cm rock fragments compared to the 3.81 cm rock fragments. This is possibly due to the greater energy imposed for the large-scale testing. All tested sandstones were found to be sensitive to immersion into water. Khok Kruat sandstone shows the greatest water-sensitivity of about 12%. The laboratory degradation simulation can accelerate the weight loss about 18 times faster than that under field condition. This is indicated by the fact that the amount of water absorption for laboratory-simulated specimens increase at a more rapid rate (about 18 times higher) than that under the actual condition (Figure 12). As a result the weight loss for the laboratory-simulated specimens is about twice as fast as that under in-situ condition (Figure 13). The decrease of the sandstone density with time under the two conditions however is not much different (Figure 14). The differences of the elastic moduli of the two conditions are

Table 9. Uniaxial compressive strengths and elastic moduli of rocks for degradation simulation under actual condition.

Days	Uniaxial Compressive Strength (MPa)			Elastic Modulus (GPa)		
	KKSS	PKSS	PWSS	KKSS	PKSS	PWSS
0	67.1±4.5	84.1±4.1	66.8±13.9	11.8±2.5	12.3±2.4	11.2±3.2
120	45.1±15.6	72.4±10.3	42.5±10.1	10.4±1.5	11.1±3.6	9.7±3.1
240	40.6±14.5	64.2±10.7	37.5±11.5	9.3±2.5	10.5±2.5	8.2±2.1
360	38.9±15.8	56.2±10.7	36.2±9.1	8.5±2.2	9.7±1.5	7.7±1.6
480	35.6±4.4	51.0±3.1	35.9±3.1	8.0±1.2	9.3±2.1	7.4±2.3

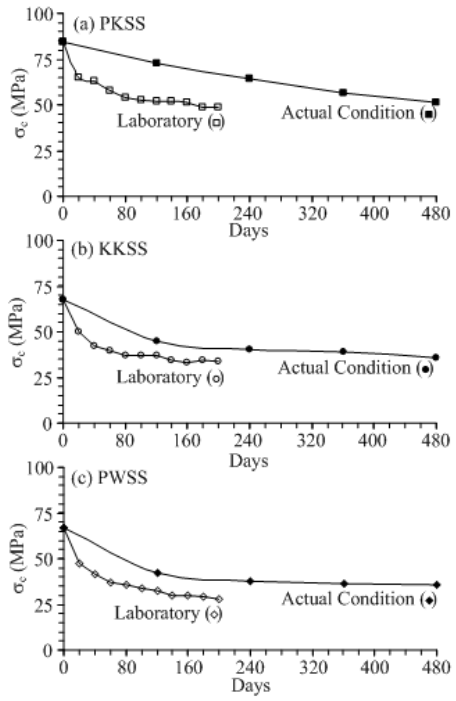

Figure 15. Compressive strength as a function of time under degradation simulation in laboratory and under actual conditions.

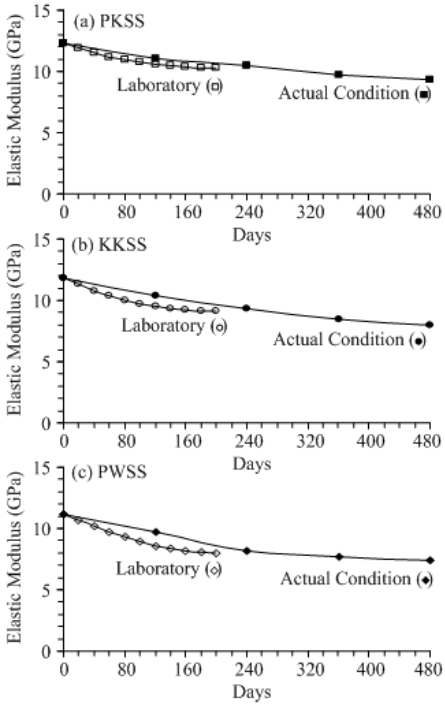

Figure 16. Elastic modulus as a function of time under degradation simulation in laboratory and under actual conditions.

less than 1 GPa. This is because of the increase of rock fissures and pore spaces due to the rock degradation that does not have much effect on the specimen weight. This implies that the degradation process is mainly caused by the physical mechanism (increase in pore spaces) not by the chemical process (mineral alteration). Both elastic modulus and compressive strength of the laboratory-simulated specimens decrease with time at a significantly rapid rate than those subject to the actual in-situ condition (Figure 15 and 16). After 200 days of laboratory degradation simulation the uniaxial compressive strengths of KK, PK and PW sandstones reduce from 67.1, 84.1and 66.8 MPa to 33.9, 48.8 and 27.6 MPa, respectively. Under 480 days of actual field condition the strengths of KK, PK and PW sandstones reduce to 35.6, 51.0, and 35.9 MPa, respectively. The decreasing rates of rock densities under the laboratory and the actual field conditions are similar. For all tested rocks the dry densities are reduced by about 0.1 g/cm^3 after 480 days of testing. These results agree well with the results from the water absorption and weight loss measurements mentioned earlier.

It can be concluded here that the results obtained from the large-scale slake durability index testing can represent rock degradation twice faster than the standard (smaller-scale) testing. The large-scale test can provide a smooth transition of weight loss from the as-collected condition through the 10 cycles of testing. The laboratory simulation of rock degradation can be correlated with in-situ conditions by subjecting to cycles of rapid cooling-heating. These results are reported here in terms of weight loss, density drop, the decrease of the uniaxial compressive strength and elasticity of the tested sandstones. The findings suggest that the rock degradation can be effectively simulated under

laboratory condition, and hence the results allow predicting the long-term degradation of the rock under the actual environment.

Acknowledgtment

This research is funded by Suranaree University of Technology and by the Higher Education Promotion and National Research University of Thailand. Permission to publish this paper is gratefully acknowledged.

References

ASTM C127-04. Standard test method for density, relative density (specific gravity), and absorption of coarse aggregate. Annual Book of ASTM Standards, Vol. 04.02. Philadelphia: American Society for Testing and Materials.

ASTM D4644-87. Standard test method for Slake durability of shale and similar weak rocks. Annual Book of ASTM Standards, Vol. 04.08. Philadelphia: American Society for Testing and Materials.

ASTM D6473-10. Standard Test Method for Specific Gravity and Absorption of Rock for Erosion Control. Annual Book of ASTM Standards, Vol. 04.08. Philadelphia: American Society for Testing and Materials.

ASTM D7012-04. Standard test method for compressive strength and elastic moduli of intact rock core specimens under varying states of stress and temperatures. Annual Book of ASTM Standards, Vol. 04.08. Philadelphia: American Society for Testing and Materials.

Brown, E.T. 1981. Rock Characterization, Testing and Monitoring – ISRM Suggested Methods. Oxford: Pergamon.

Dhakal, G., Yoneda, T., Kata, Y. and Kaneko, K. 2002. Slake durability and mineralogical properties of some pyroclastic and sedimentary rocks. Engineering Geology. 65(1), 31-45.

Fang, Z. and Harrison, J.P. 2001. A mechanical degradation index for rock. International Journal of Rock Mechanics and Mining Sciences. 38(8), 1193-1199.

Fuenkajorn, K. and Kenkhunthod, N. 2010. Influence of loading rate on deformability and compressive strength of three Thai sandstones. Geotechnical and Geological Engineering. 28(5), 707-715.

Gokceoglu, C., Ulusay, R. and Sonmez, H. 2000. Factors affecting the durability of selected weak and clay-bearing rocks from Turkey, with particular emphasis on the influence of the number of drying and wetting cycles. Engineering Geology. 57(1), 215-237.

Kemthong, R. 2006. Determination of rock joint shear strength based on rock physical properties. M.Sc. Thesis, Suranaree University of Technology, Nakhon Ratchasima Thailand.

Koncagul, E.C. and Santi, P.M. 1999. Predicting the unconfined compressive strength of the Breathitt shale using slake durability, Shore hardness and rock structural properties. International Journal of Rock Mechanics and Mining Science. 36(2), 139-153.

Oguchi, C.T. and Matsukura, Y. 1999. Effect of porosity on the increase in weathering-rind thickness of andesite gravel. Engineering Geology. 55(1-2), 77-89.

Oyama, T. and Chigira, M. 1999. Weathering rate of mudstone and tuff on old unlined tunnel walls. Engineering Geology. 5(1-2), 15-27.

Phienwej, N. and Singh, V.K. 2005. Engineering Properties of Rocks of Phu Kadung and Phra Wihan Formations in Northeast Thailand. Proceedings of the International Symposium-GEOINDO, Khon Kaen, Thailand, pp. 199-204.

Richard, E.S., Claus, B. and Gordon, J.V.W. 1998. Fundamentals of Thermodynamics. John Wiley & Sons, Singapore.

Singh, B. and Goel, R.K., 1999. Rock Mass Classification: A Practical Approach in Civil Engineering. Elsevier Science, U.K.

Sri-in, T. and Fuenkajorn, K. 2007. Slake durability index strength testing of some weak rocks in Thailand, ThaiRock 2007, September, 13-14, pp. 145-159.

Tugrul, A. 2004. The effect of weathering on pore geometry and compressive strength of selected rock types from Turkey. Engineering Geology. 75(3-4), 215-227.